Role of the pseudogap in the electron transport of quasicrystals and their approximants

1998 J. Phys.: Condens. Matter 10 4609

(http://iopscience.iop.org/0953-8984/10/21/017)

J. Phys.: Condens. Matter **10** (1998) 4609–4623. Printed in the UK PII: S0953-8984(98)88778-X

Role of the pseudogap in the electron transport of quasicrystals and their approximants

Uichiro Mizutani

Department of Crystalline Materials Science, School of Engineering, Nagoya University, Furo-cho, Chikusa-ku, Nagoya 464-01, Japan

Received 28 October 1997, in final form 16 March 1998

Abstract. There are two routes in the opening of the pseudogap: one due to the band separation in a disordered system such as expanded liquid mercury and amorphous alloys and the other due to the Fermi surface–Brillouin zone interaction in quasicrystals and their approximants. The role of the pseudogap in the electron transport has been studied by plotting resistivities at 4.2 and 300 K against the electronic specific heat coefficient for a total of 49 quasicrystals and their approximants on the log–log diagram in comparison with those for the amorphous alloys. Among them, 32 data points are for sp-electron quasicrystals and their approximants like Al–Mg–Zn, Al–Li–Cu, Mg–Zn–Ga while 17 data points are for the Mackay icosahedral-type quasicrystals like Al–Cu–Fe and Al–Cu–Ru. All the data except for the Al–Pd–Re quasicrystal of high quality are found to fall on a straight line with a slope of -2. Whether or not the data for the Al–Pd–Re quasicrystal of high quality can be treated on the same footing is left for further investigation. From this we conclude that the resistivity changes in proportion to the square of the density of states (DOS) at the Fermi level in conformity with the Mott theory for all systems characterized by the pseudogap across the Fermi level.

1. Introduction

The presence of the pseudogap across the Fermi level E_F in quasicrystals and their approximants has received strong attention both from the theoretical and experimental point of view and, particularly, attention has been focused on its possible role in lowering the electronic energy in favour of these complex electron compounds and in enhancing the electrical resistivity up to the level of doped semiconductors [1, 2]. It is, therefore, of great interest to examine how the residual resistivity is related to the depth of the pseudogap, which certainly depends on the quasicrystal chosen.

Mott [3] defined the pseudogap in a disordered system as a density of states (DOS) minimum arising from the two overlapping bands and described its depth in terms of the so called g-parameter defined as the ratio of the DOS at E_F, $N(E_F)$, over the corresponding free electron value $N(E_F)^{free}$. He argued that the transport theory based on the Boltzmann transport equation is valid when the scattering is weak, but that the conductivity decreases as g^2 when the Fermi level falls in the pseudogap and the mean free path of the conduction electron Λ_F is constrained by an average atomic distance a.

The pseudogap opens in two different routes: one due to the separation of the overlapping bands in a disordered system as in expanded liquid metals [4] and the other

0953-8984/98/214609+15$19.50

due to the Fermi surface–Brillouin zone interaction in an ordered system as in crystals and quasicrystals [1, 2]. It is certainly interesting to study whether the Mott mechanism proposed for a disordered system can be extended to quasicrystals and their approximants having the pseudogap originating from the Fermi surface–Brillouin zone interaction.

We show in this work that the role of the pseudogap in the electrical conductivity or the residual resistivity of quasicrystals and their approximants can be discussed with reference to the g-parameter in the same manner as for the sp-electron amorphous alloys and liquid metals. However, the evaluation of the g-parameter becomes difficult in the d-electron systems containing the transition metal element as a major component, since the value of $N(E_F)^{free}$ cannot be reliably estimated. In order to facilitate more universal discussion by covering both sp- and d-electron systems, we directly focus on the DOS at the Fermi level without taking its ratio over the corresponding free electron value.

Sets of the resistivity at 4.2 and 300 K and the electronic specific heat coefficient data available in the literature for icosahedral quasicrystals and their approximants, together with sp-electron amorphous alloys, are plotted on the log–log diagram. We show that the resistivity, particularly at 300 K, is inversely proportional to the square of the DOS at the Fermi level for systems having the pseudogap across the Fermi level. This universal relation is complementary to the g^2-dependence of the conductivity but holds more universally by including not only the sp-electron systems but also the d-electron systems. By making use of this universal relation, we discuss the scattering mechanism in quasicrystals and their approximants in comparison with that in amorphous alloys.

2. Test of g^2-dependence of the conductivity in sp-electron systems

According to Mott [3], the conductivity at 0 K, σ_0, is expressed as a function of the g-parameter in the form of

$$\sigma_0 = g^2 e^2 \Lambda_F S_F^{free}/12\pi^3\hbar \tag{1}$$

where S_F^{free} is the area of the free electron Fermi surface. Other symbols carry the usual meanings. The scattering probability, $1/\tau$, must be proportional to the final DOS at the Fermi level, $N(E_F)$ or the g-parameter within the second-order perturbation theory. Mott noted that the mean free path in equation (1) would be replaced by $\Lambda_F = \Lambda_F^{free}/g^2$ in the weak scattering limit, since the Fermi velocity given by $\hbar^{-1}\partial E/\partial k$ is inversely proportional to the g-parameter when the Fermi surface approaches the zone boundary in the nearly free electron approximation. Then equation (1) becomes independent of the g-parameter and is reduced to the free electron expression $\sigma_0 = e^2\Lambda_F^{free}S_F^{free}/12\pi^3\hbar$, where the mean free path Λ_F^{free} is determined by the first-order perturbation and is much longer than an average atomic distance. This means that the electron transport can be described in the context of the Boltzmann transport equation coupled with the nearly free electron model in the weak scattering limit of $\Lambda_F \gg a$. Instead, when the Fermi level falls into a deep valley of the pseudogap and the g-parameter is lowered below unity, the scattering is no longer treated in the nearly free electron approximation. This is the regime where Mott claims that the conductivity decreases as g^2 in accordance with equation (1).

Figure 1(a) and (b) reproduce the Ge concentration dependence of the resistivity at 300 K together with that of the Hall coefficient for a series of the amorphous $(Ag_{0.5}Cu_{0.5})_{100-x}Ge_x$ alloys [5–8]. The data for the electronic specific heat coefficient are included in the inset to figure 1(b). Here the corresponding free electron values calculated under the assumption that Ag, Cu and Ge atoms donate one, one and four free electrons per atom, respectively, are plotted as dashed curves. The ratio of the electronic specific heat coefficient over

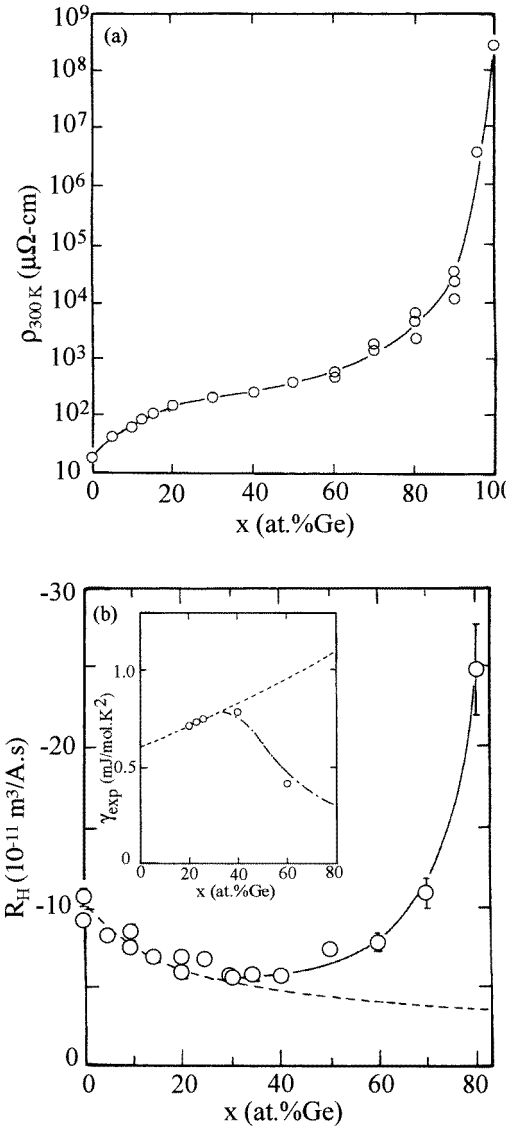

Figure 1. Ge concentration dependence of (a) the resistivity at 300 K and (b) the Hall coefficient at 300 K in the amorphous $(Ag_{0.5}Cu_{0.5})_{100-x}Ge_x$ alloys [5–8]. Inset shows that of the electronic specific heat coefficient. Dashed curves are obtained in the free electron model.

the corresponding free electron value agrees very well with that calculated from the Hall coefficient (see figure 5(a)). Hence, the g-parameter can be equally determined in this system either from the electronic specific heat coefficient or from the Hall coefficient. It is shown that the g-parameter remains unity up to $x = 30$ but decreases sharply with further increase in the Ge concentration.

The conductivity at 300 K for a series of the amorphous $(Ag_{0.5}Cu_{0.5})_{100-x}Ge_x$ alloys is plotted in figure 2 on the log–log scale against the g-parameter determined from the Hall coefficient, together with the data for expanded liquid mercury [4, 5]. The data for the

amorphous $(Ag_{0.5}Cu_{0.5})_{100-x}Ge_x$ ($x \leqslant 30$) alloys and expanded liquid mercury possessing conductivities higher than approximately 3000 Ω^{-1} cm^{-1} fall on the vertical line with $g = 1$. This is the regime to which the theory based on the Boltzmann transport equation can be applied. In contrast, the data for the amorphous $(Ag_{0.5}Cu_{0.5})_{100-x}Ge_x$ ($x \geqslant 40$) alloys and the expanded liquid mercury below about 3000 Ω^{-1} cm^{-1} are fitted to a straight line with a slope of $+2$. We see from figure 2 that, once the pseudogap appears at the Fermi level and the g-parameter is lowered below unity, the conductivity decreases in proportion to the square of the g-parameter in an excellent agreement with the Mott theory.

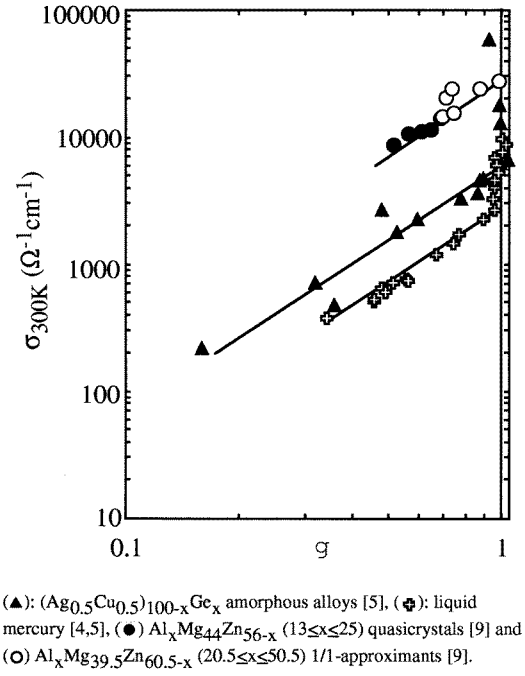

(▲): $(Ag_{0.5}Cu_{0.5})_{100-x}Ge_x$ amorphous alloys [5], (✥): liquid mercury [4,5], (●) $Al_xMg_{44}Zn_{56-x}$ (13≤x≤25) quasicrystals [9] and (○) $Al_xMg_{39.5}Zn_{60.5-x}$ (20.5≤x≤50.5) 1/1-approximants [9].

Figure 2. Conductivity as a function of the g-parameter on the log–log scales. Note that each straight line has the slope of $+2$.

Our next objective is to see whether the g^2-dependence of conductivity holds in sp-electron quasicrystals and approximants possessing the pseudogap at the Fermi level. For this particular purpose, we choose the $Al_xMg_{39.5}Zn_{60.5-x}$ 1/1-approximants ($20.5 \leqslant x \leqslant 50.5$) and $Al_xMg_{44}Zn_{56-x}$ ($13 \leqslant x \leqslant 25$) icosahedral quasicrystals, since their electronic structure, atomic structure and electron transport properties have been thoroughly studied from both experimental and theoretical approaches [9–11]. The XPS valence band studies and the electronic specific heat measurements clearly showed the existence of the pseudogap at the Fermi level in all compounds except for the 1/1-approximant containing the highest amount of Al with $x = 50.5$. Indeed, the XPS measurements revealed that the pseudogap at the Fermi level becomes apparently shallower with increasing Al concentration x and almost vanishes at $x = 50.5$ within the accuracy of the measurement. The electronic specific heat coefficient in the 1/1-approximants is found to increase with increasing Al concentration and to approach the free electron value at $x = 50.5$.

The realistic band calculations [10] have been made for a series of $Al_xMg_{40}Zn_{60-x}$ ($15 \leqslant x \leqslant 52.5$) 1/1-approximants in the framework of the LMTO–ASA method by using

the atomic structure determined by the Rietveld method [11]. It clearly demonstrated that the Fermi level moves across the pseudogap with increasing Al concentration x and almost escapes from the pseudogap at $x = 52.5$. Judging from both experimental and theoretical studies, we can assume the g-parameter for the 1/1-approximant with $x = 50.5$ to be equal to unity. The g-parameter for the remaining 1/1-approximants and quasicrystals may be evaluated by taking the ratio of the measured electronic specific heat coefficient [9] over that of the $x = 50.5$ sample. The g-parameter dependence of conductivity at 300 K thus obtained is included in figure 2. Clearly the conductivity for the Al–Mg–Zn approximants together with the quasicrystals follows well the g^2-dependence. From this we conclude that the g^2-dependence of conductivity holds, whenever the Fermi level falls in the pseudogap for either a disordered system like amorphous alloys or an ordered system like quasicrystals and their approximants.

3. $(N(E_F))^2$ dependence of the conductivity in sp- and d-electron systems

Equation (1) contains a profound implication. As noted in section 2, it is reduced to the free electron expression $\sigma_0 = e^2\Lambda_F^{free}S_F^{free}/12\pi^3\hbar$ when $g > 1$ or very close to unity. The g^2-dependence in equation (1) appears only when the Fermi level falls in the pseudogap and g is lowered below unity. The latter cannot be deduced from the nearly free electron approximation. Mott [12] demonstrated the validity of the g^2-dependence in equation (1) by employing the Kubo–Greenwood formula, which is applicable even to the strong scattering limit of $\Lambda_F \approx a$, and obtained the following conductivity formula for a Fermi gas at 0 K within the tight-binding approximation:

$$\sigma_0 = \rho_0^{-1} = \frac{\pi e^2 a^5 z I^2}{\hbar}\{N(E_F)\}^2 \tag{2}$$

where a is an average atomic distance, z is the coordination number of the constituent atom and I is the hopping integral defined as

$$I = \int \psi_i^* H \psi_j \, \mathrm{d}^3x \tag{3}$$

where ψ_i is the wave function at the site i and H is the Hamiltonian of the electron. Equation (2) claims that the conductivity at 0 K or the inverse of the residual resistivity increases with the square of the DOS at the Fermi level and that the smaller the overlap of wave functions over the nearest neighbouring atoms the lower the conductivity is. The validity of equation (2) may be tested by comparing the data for the sp-electron systems with those for the d-electron systems.

The resistivity at 300 K rather than that at 4.2 K is plotted in figure 3 against the measured electronic specific heat coefficient γ on the log–log diagram for amorphous alloys in two different families. The first family includes the amorphous $(Ag_{0.5}Cu_{0.5})_{100-x}Ge_x$ $(20 \leqslant x \leqslant 60)$ [5, 7], $(Ag_{0.5}Cu_{0.5})_{77.5}Si_{22.5}$ [13] and $Mg_{70}Zn_{30-x}Sn_x$ $(x = 0, 4, 6)$ [14] alloys. Their DOSs at the Fermi level are scarcely affected by the d states. Because of this, they are typical of the sp-electron system. The second family of the amorphous $Al_{90-x}Ni_{10}Si_x$ $(10 \leqslant x \leqslant 30)$ and $Al_{85-x}Ni_{15}Si_x$ $(15 \leqslant x \leqslant 35)$ alloys is specifically designed to have only 10–15 at.% Ni in the Al–Si amorphous matrix. Hence, a small amount of Ni–3d states coexists with the sp-electrons at the Fermi level and remains almost unchanged with varying concentration x. Thus, the two families of amorphous alloys are selected such that the d-state contribution at the Fermi level is absent in the first but is slightly present in the second one.

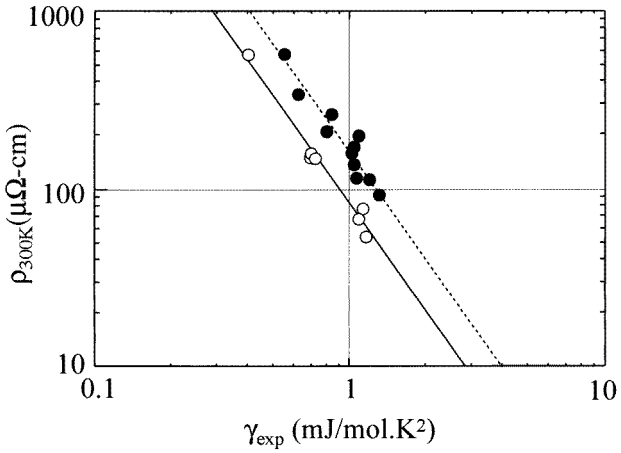

Figure 3. Resistivity at 300 K as a function of the measured electronic specific heat coefficient on the log–log scales for amorphous alloys in two different families. First family (○): $(Ag_{0.5}Cu_{0.5})_{100-x}Ge_x$ ($20 \leqslant x \leqslant 60$) [5], $(Ag_{0.5}Cu_{0.5})_{77.5}Si_{22.5}$ [13] and $Mg_{70}Zn_{30-x}Sn_x$ ($x = 0$, 4, 6) [14] alloys. Second family (●): $Al_{99-x}Ni_{10}Si_x$ ($15 \leqslant x \leqslant 35$), $Al_{85-x}Ni_{15}Si_x$ ($10 \leqslant x \leqslant 30$) and $Al_{60}Ni_{10}Ge_{30}$ [15]. Full and dashed lines having a slope of -2 are drawn to pass through the data points for the first and second families, respectively.

It is clear from figure 3 that the data for the sp-electron amorphous alloys constitute a sharp border line at the left edge with a slope of -2 in excellent agreement with equation (2). It can be also seen that the data of the second family form another parallel straight line, which is displaced to higher resistivities relative to the first one. The displacement may be explained as a reduction in the hopping integral I in equation (2) in the second family because of the mixture of the d electrons at the Fermi level. Note here that both sp and d electrons at the Fermi level contribute to the electron transport in disordered systems where the condition $\Lambda_F \approx a$ is satisfied [5].

Encouraged by the validity of the argument above, we first attempted to plot in figure 4(a) sets of the resistivity at 4.2 K and the electronic specific heat coefficient γ for a large number of icosahedral quasicrystals and their approximants [9, 16–26]. We collected the data from literature, in which both ρ and γ values are reported. The numerical data are summarized in table 1 for two families of quasicrystals and approximants: one triacontahedron-type sp-electron quasicrystals and the other Mackay icosahedral (MI) d-electron quasicrystals. The former includes those consisting of only simple elements like Al–Mg–Zn, Al–Mg–Ag, Al–Li–Cu and Mg–Zn–Ga and generally possesses resistivities lower than 1000 $\mu\Omega$ cm. A total of 32 data points for sp-electron quasicrystals and their approximants are employed. As shown in figure 4(a), the data points for sp-electron quasicrystals and their approximants are well fitted to a universal line with a slope of -2. It is also noted that the data for the amorphous $(Ag_{0.5}Cu_{0.5})_{100-x}Ge_x$ ($20 \leqslant x \leqslant 60$) alloys [5] plotted for comparison are fitted to the same universal line. This confirms that the sp-electron quasicrystals and their approximants satisfy the $\sigma_0 \propto (N(E_F))^2$ relation very well, together with the sp-electron amorphous alloys. It is noted that the g-parameter dependence of the conductivity shown in figure 2 is specific to each sp-electron system but that the data points in figure 4(a) fall on a universal line for all sp-electron systems.

A total of 17 data points are plotted in figure 4(a) for the MI-type quasicrystals. These data points fall in the resistivity range above about 1000 $\mu\Omega$ cm and clearly deviate upward

Table 1. Electronic specific heat coefficient and resistivities at 4.2 and 300 K for sp-electron quasicrystals and their approximants and for Mackay icosahedral quasicrystals and approximants.

System	γ (mJ mol^{-1} K^{-2})	$\rho_{4.2\ K}$ ($\mu\Omega$ cm)	$\rho_{300\ K}$ ($\mu\Omega$ cm)	Reference
sp-electron quasicrystals				
$Al_{25}Mg_{44}Zn_{31}$	0.99	98	92	[9]
$Al_{20}Mg_{44}Zn_{36}$	0.92	102	96	
$Al_{16}Mg_{44}Zn_{40}$	0.77	132	123	
$Al_{15}Mg_{44}Zn_{41}$	0.77	128	120	
$Al_{13}Mg_{44}Zn_{43}$	0.85	104	98	
$Al_{50.5}Mg_{39.5}Zn_{10}$ (FK)[a]	1.48	32	38	
$Al_{45.5}Mg_{39.5}Zn_{15}$ (FK)	1.33	38	44	
$Al_{40.5}Mg_{39.5}Zn_{20}$ (FK)	1.11	39	44	
$Al_{35.5}Mg_{39.5}Zn_{25}$ (FK)	1.07	47	52	
$Al_{30.5}Mg_{39.5}Zn_{30}$ (FK)	1.13	61	67	
$Al_{25.5}Mg_{39.5}Zn_{35}$ (FK)	1.06	69	73	
$Al_{20.5}Mg_{39.5}Zn_{40}$ (FK)	1.04	74	76	
$Al_{42}Mg_{44}Pd_{14}$	0.62	238	221	[16]
$Al_{46}Mg_{40}Pd_{14}$	0.71	228	218	
$Al_{50}Mg_{36}Pd_{14}$ (FK)	0.81	226	217	
$Al_{75}Cu_{15}V_{10}$	1.07	102	107	[18]
$Al_{52.4}Cu_{12.6}Mg_{35}$	1.1	65	68	
$Al_{25}Mg_{37.5}Zn_{37.5}$	0.92	76	79	
$Al_{20}Mg_{70}Ag_{10}$	1.17	81	78	[19]
$Al_{40}Mg_{50}Ag_{10}$	1.15	93	90	
$Al_{50}Mg_{30}Ag_{20}$	1.08	115	111	
$Al_{51.9}Mg_{35.8}Cu_{12.3}$	1.15	∼69	70	
$Al_{48.2}Mg_{39.5}Cu_{12.3}$	1.19	∼80	81	
$Al_{44.5}Mg_{43.2}Cu_{12.3}$	1.17	∼84	86	
$Al_{54.0}Mg_{39.5}Cu_{6.5}$	1.38	∼63	65	
$Al_{51.1}Mg_{39.5}Cu_{9.4}$	1.17	∼71	72	
$Al_{45.3}Mg_{39.5}Cu_{15.2}$	1.11	∼87	88	
$Mg_{39.5}Zn_{40.0}Ga_{20.5}$	0.99	154	143	
$Mg_{33.5}Zn_{40.0}Ga_{26.5}$	0.91	154	154	
$Mg_{36.5}Zn_{43.0}Ga_{20.5}$	0.82	172	157	
$Mg_{33.5}Zn_{46.0}Ga_{20.5}$	0.8	201	183	
$Al_{55}Li_{35.8}Cu_{9.2}$	0.318	870	800	[20]
MI quasicrystals				
$Al_{52.5}Mg_{20}Pd_{27.5}$ (MI)	0.65	605	550	[17]
$Al_{52}Mg_{18}Pd_{30}$ (MI)	0.43	798	700	
$Al_{62.5}Cu_{26.5}Fe_{11}$	0.32	3700	2280	[21]
$Al_{63.5}Cu_{24.5}Fe_{12}$	0.31	4350	2980	
$Al_{62.5}Cu_{26.5}Fe_{11}$ r phase	0.25	5550	3450	
$Al_{63}Cu_{25}Fe_{12}$	0.4	4375	2480	[22]
$Al_{63}Cu_{25}Fe_{12}$	0.345	4930	2793	
$Al_{65}Cu_{20}Ru_{15}$	0.11	13 330	4677	[21]
$Al_{64.5}Cu_{20}Ru_{15}Si_{0.5}$	0.27	5550	2775	
$Al_{64}Cu_{20}Ru_{15}Si_{1}$	0.21	3570	1950	
$Al_{65}Cu_{20}Ru_{15}$	0.11	26 000	6500	[23]
$Al_{70}Cu_{15}Ru_{15}$	0.2	10 000	4400	
$Al_{68}Cu_{17}Ru_{15}$	0.23	5600	2800	
$Al_{70.5}Pd_{21}Re_{8.5}$	0.11	1000 000	16 000	[24]
$Al_{70.5}Pd_{21}Re_{8.5}$	0.15	450 000[b]	5 625[b]	[25]
$Al_{67}Pd_{23}Re_{10}$	0.25	10 000	3030	[26]
$Al_{69}Pd_{19}Re_{12}$	0.28	1000	833	

[a] FK stands for the Frank–Kasper compound and corresponds to the 1/1–1/1–/1 approximant to the quasicrystals in this family.

[b] The resistivity value at 4 K and the ratio $\rho_{4\ K}/\rho_{300\ K}$ are reported in the thesis [25] to be 450 000 $\mu\Omega$ cm and 80, respectively, for which the γ value was measured.

from the line drawn through the sp-electron quasicrystals and their approximants. The data for the Al–Cu–Fe [21, 22] and Al–Cu–Ru [21, 23] quasicrystals may be fitted to another straight line with a slope of -2. This may be explained in the same way as that discussed in relation to figure 3, since the MI-type quasicrystals contain significant amounts of transition metals as constituent elements. However, the situation in the almost insulating Al–Pd–Re quasicrystal of high quality [24, 25] may be different.

The Al–Pd–Re quasicrystals are known to possess the highest resistivity in quasicrystals so far reported and have been discussed as being marginal to the metal–insulator transition [24–26]. Admittedly, however, the value of the resistivity at 4.2 K for the Al–Pd–Re quasicrystal sensitively depends on quality and composition. As can be seen from figure 4(a), the resistivity data at 4.2 K for the Al–Pd–Re quasicrystals of high quality [24, 25] deviate further upward from the second universal line. This may be taken as an indication that the Al–Pd–Re quasicrystal is no longer in the metallic regime.

Some caution is exercised in the analysis of the ρ–γ data for the MI-type quasicrystals with resistivities as high as 100 000 $\mu\Omega$ cm–1 Ω cm in figure 4(a). In such a high resistivity regime, the electronic specific heat coefficient γ becomes very low. The measured value of γ may not represent the DOS at the Fermi level when it is reduced to the order of 0.1 mJ mol K^{-2}. Here the contributions of the electron–phonon mass enhancement and the two-level tunnelling effect may be properly subtracted to deduce the DOS at the Fermi level.

A more serious difficulty stems from the choice of the resistivity at 4.2 K. The quantum interference effect including the weak localization coupled with the enhanced electron–electron interaction participates at such low temperatures in the strong scattering limit where $\Lambda_F \approx a$. The Mott theory is certainly irrelevant to it. Hence, $\rho_{4.2\ \mathrm{K}}$ may not be chosen as an appropriate quantity to examine the applicability of the Mott theory to such high resistivity quasicrystals. Since the quantum interference effect diminishes with increasing temperature, we consider it to be worthwhile constructing the ρ–γ diagram by using the resistivity at 300 K rather than the value at 4.2 K.

Figure 4(b) is constructed by replacing $\rho_{4.2\ \mathrm{K}}$ in figure 4(a) by the corresponding value at 300 K, $\rho_{300\ \mathrm{K}}$. Note here that the deviation of the ratio $\rho_{4.2\ \mathrm{K}}/\rho_{300\ \mathrm{K}}$ from unity for the sp-electron quasicrystals with resistivities less than 1000 $\mu\Omega$ cm is always less than 10% and is so small that the data in figure 4(a) in this regime remain essentially unaffected. However, the ratio is over 2 for the Al–Cu–Fe and Al–Cu–Ru quasicrystals [21] and even reaches 5–80 for the Al–Pd–Re quasicrystals [24–26]. As a consequence, the data points for the MI-type quasicrystals are lowered in the ρ–γ diagram and happen to be closely distributed along the universal line drawn through the sp-electron quasicrystals. This is indeed surprising and may be indicative that the resistivity at 300 K, which is essentially free from the quantum interference effect, obeys the Mott theory well and that a still existing small upward deviation from the universal line for the Mackay-type quasicrystals is due to the difference in the hopping integral between sp-electron and d-electron systems. But further work is certainly needed to make this argument more decisive.

The reservation for this is that the discussion of the electron transport mechanism on the ρ–γ diagram is meaningful only for metallic systems, where the Fermi cut-off is well defined and the DOS at the Fermi level is finite at 0 K. A choice of the room temperature resistivity would make a clear differentiation of metallic and insulating systems more difficult. Moreover, the electron transport mechanism including the evaluation of the contribution of the quantum interference effect in high resistivity quasicrystals has not been well elucidated. For example, the temperature dependence of the conductivity for the Al–Pd–Re quasicrystal of high quality is experimentally found to follow the power law

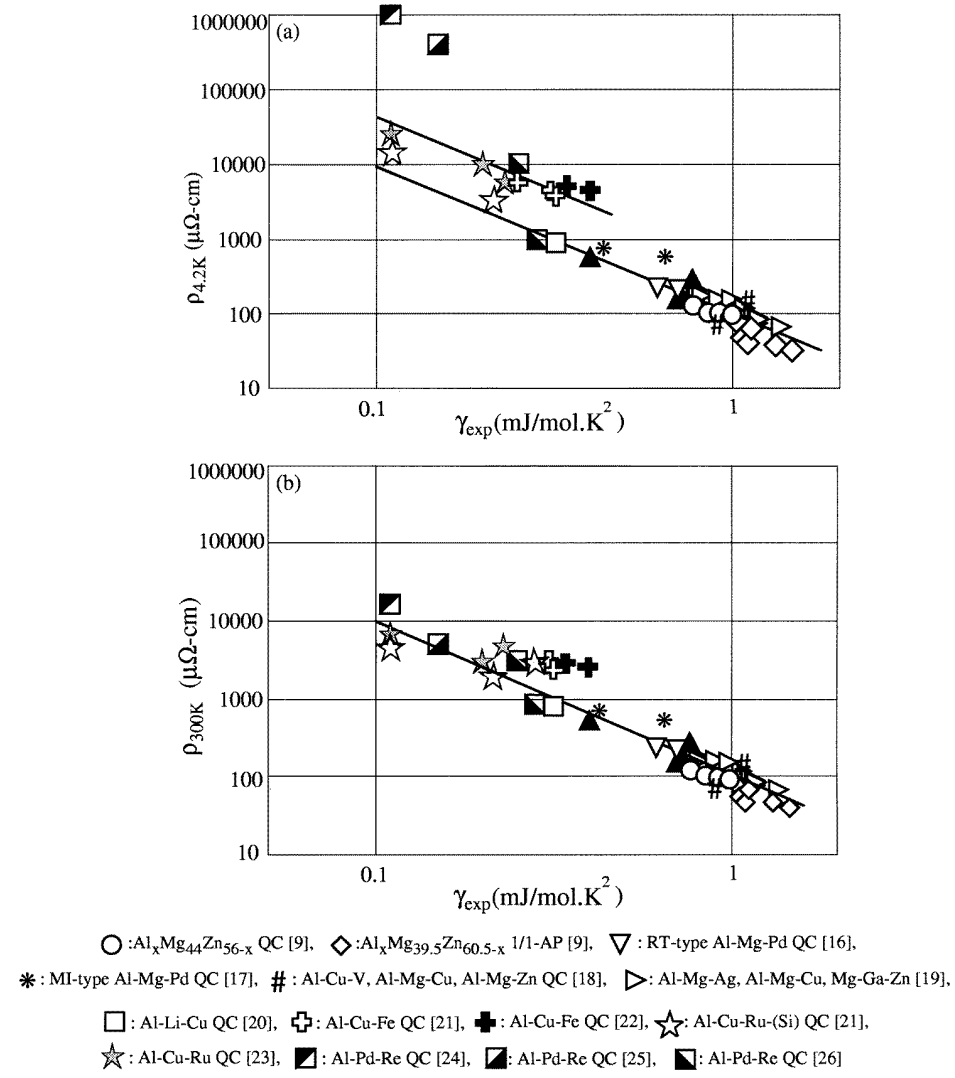

Figure 4. Resistivity at (a) 4.2 and (b) 300 K as a function of the measured electronic specific heat coefficient on the log–log diagram for quasicrystals and their approximants. The data (▲) for the amorphous Ag–Cu–Ge alloys shown in figure 3 are also included. A line with a slope of −2 is drawn as a guide. The data of Al–Cu–Li and Ga–Mg–Zn in [18] are deliberately omitted because of too large deviation from the universal line.

$\sigma(T) \propto T^{1.13}$ over a wide temperature range 0.3–600 K [25]. But no clear interpretation has been put forward to explain this unique power law temperature dependence.

4. Comparison of the electron transport properties between amorphous alloys and quasicrystals

We have so far shown that the pseudogap at the Fermi level gives rise to the $\sigma_0 \propto (N(E_F))^2$ relation, being apparently independent of the mechanism for its formation. In this section, we

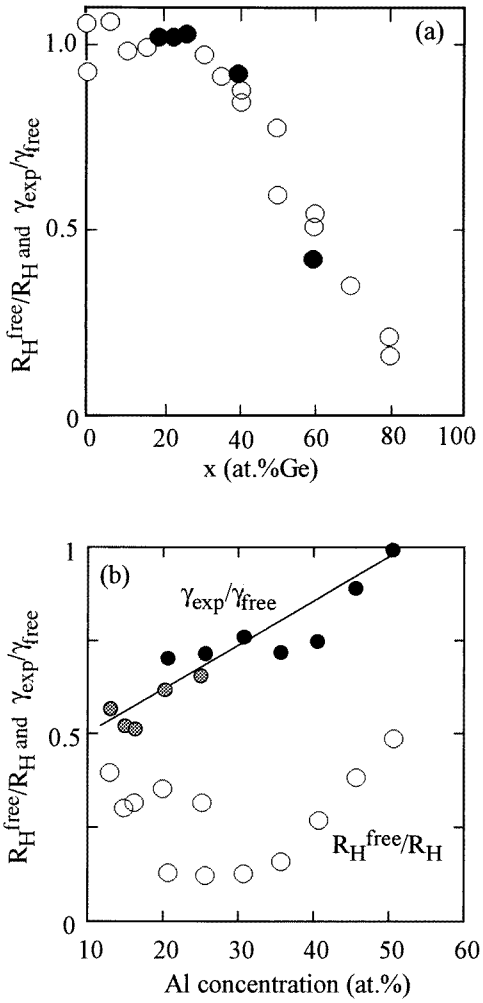

Figure 5. Ratio of the free electron Hall coefficient over the measured Hall coefficient R_H^{free}/R_H (○) and the ratio of the measured electronic specific heat coefficient over the free electron value $\gamma_{exp}/\gamma_{free}$ (●) for (a) amorphous $(Ag_{0.5}Cu_{0.5})_{100-x}Ge_x$ ($0 \leqslant x \leqslant 95$) alloys [5] and (b) the $Al_xMg_{39.5}Zn_{60.5-x}$ ($20.5 \leqslant x \leqslant 50.5$) 1/1-approximants and $Al_xMg_{44}Zn_{56-x}$ ($13 \leqslant x \leqslant 25$) quasicrystals [9]. The grey circles are used for the quasicrystals.

attempt to extract more specific features in the electron transport properties of quasicrystals and their approximants in comparison with those for amorphous alloys typical of a disordered system.

4.1. The Hall coefficient

The ratio of the free electron Hall coefficient over the measured one R_H^{free}/R_H for the amorphous $(Ag_{0.5}Cu_{0.5})_xGe_{100-x}$ alloys [8] is plotted in figure 5(a) as a function of Ge concentration, together with the ratio of the measured electronic specific heat coefficient over the corresponding free electron value [5]. An excellent agreement can be seen between the two sets of data. Indeed we have employed in figure 2 the ratio of the free electron Hall

coefficient over the measured one as the g-parameter in the amorphous $(Ag_{0.5}Cu_{0.5})_xGe_{100-x}$ alloys. In the case of the Al–Mg–Zn quasicrystals and their approximants, the ratio of the electronic specific heat coefficient over that of the approximant with $x = 50.5$ can be used as the g-parameter, as explained in section 2. What about the ratio of the Hall coefficient?

The R_H^{free}/R_H data for the Al–Mg–Zn quasicrystals and 1/1-approximants [9] are plotted in figure 5(b) as a function of the Al concentration. It is clear that the ratio of the Hall coefficient no longer coincides with the g-parameter derived from the electronic specific heat coefficient. This is in sharp contrast to the data for the amorphous $(Ag_{0.5}Cu_{0.5})_xGe_{100-x}$ alloys. The absence of sharp Brillouin zones in amorphous alloys must be responsible for the agreement of the ratio of the Hall coefficient with the g-parameter derived from the electronic specific heat coefficient. Instead, the quasicrystals and their approximants possess the anisotropic electronic structure consisting of many small electron and hole Fermi surfaces because of the presence of a large number of Brillouin zone planes [27]. If the carrier densities of the electrons and holes can be calculated with a reasonable accuracy from the Fermi surface thus obtained, then the application of the two-band model would explain the breakdown of the correlation between the observed ratio R_H^{free}/R_H and the g-parameter.

4.2. Temperature dependence of the electrical resistivity

As discussed in section 3, the Al–Pd–Re quasicrystal of high quality is marginal to the metal–insulator transition and the temperature dependence of its conductivity obeys a unique power law over a wide temperature range. Apart from such complex transport behaviour in an extremely high resistivity regime, the electron transport mechanism of quasicrystals in the low resistivity regime is also interesting. Here we focus on the resistivity behaviour of the Al–Mg–Zn quasicrystals and their approximants in comparison with that of the amorphous $(Ag_{0.5}Cu_{0.5})_{100-x}Ge_x$ alloys, particularly in the range $0 \leqslant x \leqslant 30$.

As shown in figure 1, the resistivity for the amorphous $(Ag_{0.5}Cu_{0.5})_{100-x}Ge_x$ alloys increases from about 20 to 200 $\mu\Omega$ cm with increasing Ge concentration in the range $x = 0$–30. The temperature dependence of the electrical resistivity for the amorphous $(Ag_{0.5}Cu_{0.5})_{100-x}Ge_x$ alloys [7] is reproduced in figure 6(a). It has been argued [5, 28] that the temperature dependence of the resistivity shown in figure 6(a) can be interpreted within the framework of the Boltzmann transport equation into which the electron–phonon interaction is incorporated and that the unique concentration dependence of the temperature dependence of resistivity marked as types (a) to (c) reflects the decreasing mean free path from above 20 Å down to a value comparable to the average atomic distance of about 4 Å. This means that the condition $\Lambda_F > a$ is well satisfied. In addition, the g-parameter in the range $x = 0$–30 is experimentally determined to be unity. Therefore, the scattering involved in the amorphous $(Ag_{0.5}Cu_{0.5})_{100-x}Ge_x$ alloys in the range $0 \leqslant x \leqslant 30$ can be treated in the nearly free electron model without invoking the quantum interference effect in excellent agreement with the Mott theory.

Resistivities of the $Al_xMg_{39.5}Zn_{60.5-x}$ ($20.5 \leqslant x \leqslant 50.5$) 1/1 approximants and $Al_xMg_{44}Zn_{56-x}$ ($13 \leqslant x \leqslant 25$) icosahedral quasicrystals are distributed over the range 40–150 $\mu\Omega$ cm [9], being the same magnitudes as those of the amorphus $(Ag_{0.5}Cu_{0.5})_{100-x}Ge_x$ ($0 \leqslant x \leqslant 30$) alloys. As shown in figure 6(b), its temperature dependence is also very similar to that for the amorphous $(Ag_{0.5}Cu_{0.5})_{100-x}Ge_x$ ($0 \leqslant x \leqslant 30$) alloys. Indeed, the TCR (temperature coefficient of resistivity) changes its sign from a positive to a negative value with increasing resistivity in both systems. Therefore, as far as the resistivity behaviour is concerned, no discernible difference can be seen between

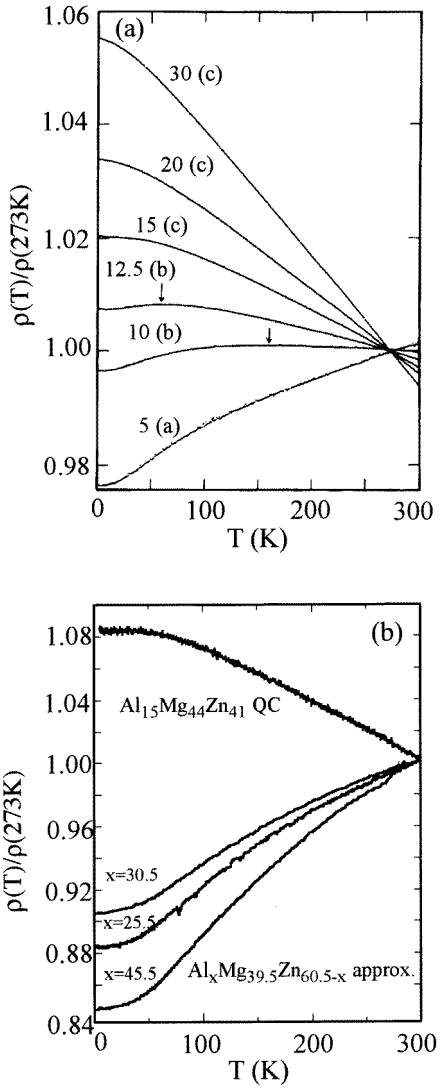

Figure 6. Temperature dependence of the electrical resistivity for (a) amorphous $(Ag_{0.5}Cu_{0.5})_{100-x}Ge_x$ ($0 \leqslant x \leqslant 30$) alloys [5–7] and (b) the $Al_xMg_{39.5}Zn_{60.5-x}$ (25.5, 30.5 and 45.5) 1/1-approximants and $Al_{15}Mg_{44}Zn_{41}$ quasicrystal [9]. Letters in the brackets in (a) mark the ρ–T types (see its definition in [5]) and the arrow indicates the maximum in resistivity.

these two systems. However, there exists a sharp difference in the electronic structure at the Fermi level between them. As has been discussed, the Al–Mg–Zn quasicrystals and their 1/1-approximants possess the pseudogap characterized by the g-parameter in the range $0.6 < g < 1$ in sharp contrast to the possession of $g = 1$ for the amorphous $(Ag_{0.5}Cu_{0.5})_{100-x}Ge_x$ ($0 \leqslant x \leqslant 30$) alloys.

It is, therefore, interesting to discuss the reason for the absence of the quantum interference effect in the $Al_xMg_{39.5}Zn_{60.5-x}$ ($20.5 \leqslant x \leqslant 50.5$) 1/1-approximants in spite of the possession of the pseudogap at the Fermi level. The mean free path of conduction electrons for the 1/1-approximants is estimated to be 15–20 Å by inserting into the Drude

expression $\rho_0^{-1} = (e^2/3)\Lambda_F v_F N(E_F)$ the residual resistivity and the electronic specific heat coefficient. Here the Fermi velocity v_F is estimated as g times the free electron value, since the conductivity in this system is scaled in terms of g^2, as shown in figure 2. The mean free path of the conduction electron thus obtained is much longer than an average atomic distance and is even slightly longer than the lattice constant of 14.2 Å in the 1/1-approximant. Thus, conduction electrons are still able to recognize the periodicity of the lattice in the 1/1-approximant. This is the reason for the absence of the quantum interference effect and, instead, for the validity of the discussion based on the Boltzmann transport equation for the $Al_xMg_{39.5}Zn_{60.5-x}$ 1/1-approximants, despite the fact that the pseudogap exists at the Fermi level.

Before ending this section, we direct our attention once again to the data shown in figure 2, where the effect of the mean free path on the electron conduction is manifested. The data for the three different systems can be fitted to their own g^2-dependent straight lines. The values of their intercepts with the $g = 1$ vertical line can be read off from figure 2 as 25 000, 5000 and 3000 Ω^{-1} cm^{-1} for the Al–Mg–Zn approximants, the amorphous $(Ag_{0.5}Cu_{0.5})_{100-x}Ge_x$ ($x > 30$) alloys and expanded liquid mercury, respectively. Hence, the ratio of the conductivity of the approximant over that of the amorphous alloy is found to be equal to five. Note that the mean free path of the conduction electron for the amorphous $(Ag_{0.5}Cu_{0.5})_{100-x}Ge_x$ alloys, when x exceeds 30, has been calculated to be about 4 Å, whereas that for the Al–Mg–Zn approximants is 15–20 Å. Therefore, the ratio of the mean free paths of the conduction electron of the approximant over that of the amorphous alloy coincides well with the ratio of the intercepts above. In other words, the appearance of three different g^2-dependent straight lines in figure 2 indicates that each system possesses its own mean free path.

The data for the expanded liquid mercury are located below those for the amorphous $(Ag_{0.5}Cu_{0.5})_{100-x}Ge_x$ alloys. This suggests the mean free path of the conduction electron in the former to be shorter than that in the latter. We consider this to be plausible, since only a single element is involved in liquid mercury as a constituent element. Indeed, an average atomic distance for the expanded liquid mercury turns out to be 3 Å from the measured density [4] of 11 g cm^{-3}. A shorter mean free path than that in the amorphous $(Ag_{0.5}Cu_{0.5})_{100-x}Ge_x$ alloys with $x > 40$ would be responsible for the lower location of the data for the expanded liquid mercury.

5. Universal relation $\sigma_0 \propto (N(E_F))^2$ versus spiky peaks in calculated DOS

Band calculations so far made for various approximants are consistent with the findings of the pseudogap across the Fermi level together with a number of spiky peaks in the DOS spectrum [10, 27, 29, 30]. The latter originates from fairly flat energy dispersions as a result of the folding into small first Brillouin zone. The presence of the pseudogap has been confirmed by many experiments including the present work. However, the experimental confirmation of the spiky peaks has been controversial. A narrow dip of about 50 meV width was detected across E_F in several quasicrystals by means of scanning tunnelling spectroscopy (STS) and ascribed to the valley formed by the neighbouring spiky peaks [31]. In contrast, photoemission spectroscopy measurements with a high resolution of 5 meV have failed to detect the spiky peaks in the valence band spectra for well qualified quasicrystals cooled to 12 K [32].

As mentioned in section 2, the band calculations for the $Al_xMg_{39.5}Zn_{60.5-x}$ ($20.5 \leqslant x \leqslant 50.5$) 1/1-approximants [10] were made by using the atomic structure determined by the x-ray Rietveld analysis [11]. The resulting spiky peaks are rather wide because of the lack

of d states near the Fermi level and their width ranges over 50–100 meV. It is easily checked that the calculated DOS at the Fermi level or the electronic specific heat coefficient varies over 0.85–1.46 mJ mol K^{-2}, depending on whether the Fermi level falls at the bottom of the neighbouring spiky peaks or at the top of the peak within the energy range of 100 meV. Thus, spiky peaks had to be smoothed out in the calculated DOS to obtain a systematic Al concentration dependence of the γ value. A good agreement with the observed γ values was achieved only after smoothing. This means that only smoothed DOS is apparently measured.

In the present studies, we have established the DOS square dependence of the resistivity for a large number of quasicrystals and their approximants. This is taken as another evidence that these two quantities are indeed well defined for given quasicrystals and approximants and reflect only the smoothed pseudogap at the Fermi level. Otherwise, the data would have scattered on the ρ–γ diagram and have shown no universal relation. We believe that the present results lend support to the observation of the smoothed DOS at the Fermi level in both quasicrystals and their approximants.

The presence of chemical disordering has been emphasized in the atomic structure analysis of the 1/1-approximants [11, 33]. Such chemical disordering is ignored in the band calculations mentioned above [10]. We consider the composition fluctuations inherent in quasicrystals and their approximants even of high quality to be partly responsible for observing smoothed DOS at the Fermi level. A use of a massive sample for measurements like specific heat, resistivity and photoemission spectroscopy also contributes to averaging the fine structure of the DOS. The spikiness of the DOS may be observed only when the electronic structure is studied by an atomic-scale probe like the STS or perhaps electron energy loss spectroscopy (EELS) with the resolution better than 50 meV.

6. Conclusion

We have constructed the ρ–γ diagram for a total of 49 quasicrystals and their approximants together with sp-electron amorphous alloys, all of which are characterized by the possession of the pseudogap at E_F, and proved that the resistivity particularly at 300 K obeys well the relation $\rho \propto (N(E_F))^{-2}$ in excellent agreement with the Mott theory. Here the Al–Pd–Re quasicrystal of high quality is excluded from this universal rule at the moment. Further detailed experimental and theoretical work for the MI-type icosahedral quasicrystals, particularly the Al–Pd–Re, must be pursued along this line. The electron transport mechanism of the sp-electron quasicrystals is discussed in comparison with that of sp-electron amorphous alloys by focusing on the absence of the correlation between the observed ratio R_H^{free}/R_H and the g-parameter and the temperature dependence of the electrical resistivity over the range 2–300 K. It is also emphasized that the present results are consistent with the observation of the smoothed pseudogap at the Fermi level obtained after averaging the spiky peaks in the calculated DOS.

Acknowledgments

The author wishes to thank Dr E Belin-Ferré, Laboratoire de Chimie Physique Marie et Rayonnement, URA CNRA 176, Paris, Dr J C Lajaunias, CNRS, Grenoble, and Professor H Sato, Aichi University of Education, for valuable discussions during the course of this study.

References

[1] Kimura K and Takeuchi S 1991 *Quasicrystals: the State of the Art* ed D P Vincenzo and P Steinhardt (Singapore: World Scientific) p 313
[2] Poon S J 1992 *Adv. Phys.* **41** 303
[3] Mott N F 1969 *Phil. Mag.* **19** 835
[4] Even U and Jortner J 1972 *Phys. Rev. Lett.* **28** 31
[5] Mizutani U 1993 *Phys. Status Solidi* b **176** 9
[6] Mizutani U 1993 *Mater. Sci. Eng.* B **19** 82
[7] Mizutani U, Sato K, Sakamoto I and Yonemitsu K 1988 *J. Phys. F: Met. Phys.* **18** 1995
[8] Sakamoto I, Yonemitsu K, Sato K and Mizutani U 1988 *J. Phys. F: Met. Phys.* **18** 2009
[9] Takeuchi T and Mizutani U 1995 *Phys. Rev.* B **52** 9300
[10] Mizutani U, Iwakami W and Fujiwara T 1997 *Proc. 6th Int. Conf. on Quasicrystals (Tokyo, 1997)* ed S Takeuchi and T Fujiwara, pp 579–82
[11] Mizutani U, Iwakami W, Takeuchi T, Sakata M and Takata M 1997 *Phil. Mag. Lett.* **76** 349
[12] Mott N F 1972 *Phil. Mag.* **26** 1015
[13] Mizutani U and Yoshino K 1984 *J. Phys. F: Met. Phys.* **14** 1179
[14] Mizutani U and Matsuda T 1984 *J. Phys. F: Met. Phys.* **14** 2995
[15] Yamanaka E, Yamada Y, Ohara I, Matsuda T and Mizutani U 1988 *Proc. Int. Symp. on Non-Equilibrium Solid Phases of Metals and Alloys (Kyoto, 1988) JIM Trans. Suppl.* **29** 329
[16] Yamaguchi S, Takeuchi T, Yamada Y and Mizutani U 1995 *Proc. 5th Int. Conf. on Quasicrystals (Avignon, 1995)* ed C Janot and R Mosseri pp 548–51
Hashimoto K, Yamada Y, Yamauchi T, Tanaka T, Matsuda T and Mizutani U 1994 *Mater. Sci. Eng.* A **181/182** 785–9
[17] Mizutani U, Yamada Y, Takeuchi T, Hashimoto K, Belin E, Sadoc A, Yamauchi T and Matsuda T 1994 *J. Phys.: Condens. Matter* **6** 7335
[18] Wagner J L, Wong K M and Poon S J 1989 *Phys. Rev.* B **39** 8091
[19] Mizutani U, Sakabe Y and Matsuda T 1990 *J. Phys.: Condens. Matter* **2** 6153
[20] Kimura K, Iwahashi H, Hashimoto T, Takeuchi S, Mizutani U, Ohashi S and Itoh G 1989 *J. Phys. Soc. Japan* **58** 2472
[21] Pierce F S, Bancel P A, Biggs B D, Guo Q and Poon S J 1993 *Phys. Rev.* B **47** 5670
[22] Lasjaunias J C, Calvayrac Y and Yang H 1997 *J. Physique* I **7** 1
[23] Biggs B D, Poon S J and Munirathnam N R 1990 *Phys. Rev. Lett.* **65** 2700
[24] Pierce F S, Guo Q and Poon S J 1994 *Phys. Rev. Lett.* **73** 2220
Pierce F S, Poon S J and Guo Q 1993 *Science* **261** 737
[25] Gignoux C 1977 *PhD Dissertation* de l'Universite Joseph Fourier–Grenoble I
Berger C, Ginoux G, Wagner T, Grenet T, Fourcaudot G, Grieco J C, Calvayrac Y and Lasjaunias J C 1996 *Proc. 9th Int. Conf. on Rapidly Quenched Materials (Bratislava, 1996)*
[26] Takeuchi T, Yamada Y, Mizutani U, Honda Y, Edagawa K and Takeuchi S 1996 *Proc. 5th Int. Conf. on Quasicrystals (Avignon 1996)* ed C Janot and R Mosseri, pp 534–8
[27] Fujiwara T 1997 *Proc. 6th Int. Conf. on Quasicrystals (Tokyo, 1997)* ed S Takeuchi and T Fujiwara, pp 591–4
[28] Hafner J 1985 *J. Non-Cryst. Solids* **69** 325
[29] Trambly de Laissardière G and Fujiwara T 1994 *Phys. Rev.* B **50** 5999
[30] Krajci M, Windisch M, Hafner J, Kresse G and Mihalkovic M 1995 *Phys. Rev.* B **51** 17 355
[31] Davydov D N, Mayou D, Berger C, Ginoux C, Neumann A, Jansen A G M and Wyder P 1996 *Phys. Rev. Lett.* **77** 3173
[32] Stadnik Z M, Purdie D, Garnier M, Baer Y, Tsai A-P, Inoue A, Edagawa K, Takeuchi S and Buschow K H J 1997 *Phys. Rev.* B **55** 10 938
[33] Yamada H, Iwakami W, Takeuchi T, Mizutani U, Takata M, Yamaguchi S and Matsuda T 1997 *Proc. 6th Int. Conf. on Quasicrystals (Tokyo, 1997)* ed S Takeuchi and T Fujiwara, pp 644–7